Time-Resolved Electron Paramagnetic Resonance Investigation of Photoinitiated Antioxidant Reaction of Vitamin C (Ascorbic Acid) with Xanthone in Aqueous Sodium Lauryl Sulfate, Hexadecyltrimethylammonium Chloride, and Triton X-100 Micelle Solutions

Keishi Ohara,* Ryo Watanabe, Yoko Mizuta, Shin-ichi Nagaoka, and Kazuo Mukai

Department of Chemistry, Faculty of Science, Ehime University, Matsuyama 790-8577, Japan

Received: May 15, 2003; In Final Form: August 8, 2003

The photoinitiated reaction between vitamin C and xanthone in sodium lauryl sulfate (SDS), hexadecyltrimethylammonium chloride (CTAC), and Triton X-100 micelle solutions at various pH was investigated by time-resolved electron paramagnetic resonance (TR-EPR). The TR-EPR spectra were explained by superimpositions of the xanthone ketyl and the vitamin C radicals, showing that a fast hydrogen abstraction reaction of the excited xanthone from vitamin C progresses around the water−oil interface region of the micelles. The EPR signal intensity of the vitamin C radical showed the notable pH dependence, which seems to be attributable to the acid−base dissociation equilibrium of vitamin C. The results suggested that the present reaction is controlled by the transportation of the excited xanthone and vitamin C to the reaction-progressing region, which is the surface or inside of the micelle, and by the difference of the reactivity between the dissociation forms of vitamin C.

Introduction

Kinetic studies of antioxidant reactions of natural antioxidants, such as vitamin E (Vit-E, α, *β*, *γ*, and *δ*-tocopherols), vitamin C (Vit-C, ascorbic acid), ubiquinols, and flavonoids, are important for understanding the protection mechanisms in not only biological systems but also foods and plastics and have been performed with great interest extensively.[1−21] It is well-known that tocopherols (TocH) are localized in biomembranes and protect membranes from lipid peroxidation.[1−6] The inhibition of peroxidation is ascribed to the hydrogen transfer from phenolic hydroxyl groups to the LOO• radicals and the production of the corresponding tocopheroxyl radical (Toc•) (reaction I),[1−3]

$$\mathrm{LOO^{\bullet} + TocH \xrightarrow{k_1} LOOH + Toc^{\bullet}} \qquad \text{(I)}$$

where LOO• and LOOH stand for a lipid peroxyl radical and the corresponding hydroperoxide, respectively. Vit-C is a water-soluble antioxidant, and reduces Toc• and regenerates TocH in the water−oil interface region of a biomembrane (reaction II).[8−10]

$$\mathrm{Toc^{\bullet} + Vit\text{-}C \xrightarrow{k_2} TocH + Vit\text{-}C^{\bullet}} \qquad \text{(II)}$$

Several kinetic studies have been performed for the free-radical-scavenging reactions of Vit-E and Vit-C, using a stopped-flow technique.[11−18] The deuterium kinetic-isotope effects on the second-order reaction rate constants have been studied for reactions I and II, and the mechanism of the proton-tunneling following the partial electron transfer has been proposed.[19−21]

In previous reports,[14−16,22] the second-order rate constants (k_2) for the reaction of Vit-C with tocopheroxyl and 2,6-di-*tert*-butyl-4-(4′-methoxyphenyl)phenoxyl (ArO•) radicals were measured in homogeneous organic solvents and aqueous Triton X-100 (TX-100) micelle solutions by using the stopped-flow method. A notable pH dependence of the k_2 value was observed for the reaction in the micelle solution; the k_2 value showed a broad maximum around pH 8, and the good correlation between the k_2 and the mole fraction of the monoanion form of ascorbic acid (ascorbate monoanion, AsH^-) in the acid−base dissociation equilibrium (Figure 1) was found. The k_2 value for the regeneration reaction of 5,7-diisopropyltocopherol by Vit-C in the aqueous micelle solution was reported to be 2.49×10^3 M (mol dm^{-3})$^{-1}$ s^{-1} at pH 7. On the other hand, the k_2 value for sodium ascorbate in 2-propanol/H_2O (5:1, v/v) mixed solvent

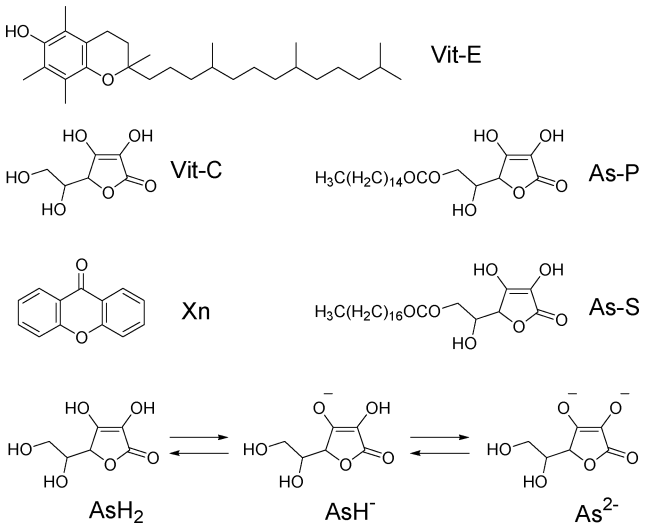

Figure 1. Molecular structures of vitamin E (Vit-E, α-tocopherol), ascorbic acid (Vit-C, AsH_2, AsH^-, As^{2-}), L-ascorbyl 6-palmitate (As−P), L-ascorbyl 6-stearate (As−S), and xanthone (Xn). The dissociation equilibrium for Vit-C is also shown.

* Corresponding author. E-mail: ohara@chem.sci.ehime-u.ac.jp.

10.1021/jp0353486 CCC: $25.00
Published on Web 09/24/2003

was 6.32×10^4 M^{-1} s^{-1}, which was 25 times as large as that in the micelle solution. Furthermore, the k_2 value for the regeneration of 7-*tert*-butyl-5-isopropyltocopherol by Vit-C in benzene/ethanol (2:1) mixtures was only 15% ($k_2 = 49$ M^{-1} s^{-1}) of that ($k_2 = 322$ M^{-1} s^{-1}) in the micelle solution at pH 7. These results suggest that the ascorbate monoanion (AsH^-) has a much larger tocopheroxyl-regeneration activity than the undissociated form of ascorbic acid (AsH_2) and ascorbate dianion (As^{2-}). The large difference in k_2 values between homogeneous and inhomogeneous systems may also suggest the importance of the material transportation to the reaction-progressing region and/or the reaction kinetics around the micelle. The pH dependence of the free-radical-scavenging rates of natural antioxidants has also been reported for the regeneration reaction of tocopheroxyl with rutin and quercetin,[22,23] which are also well-known as representative flavonoids. Therefore, the investigations on the effects of pH and inhomogeneous environments in antioxidant actions are important to discuss the detailed mechanism of the antioxidant action in inhomogeneous media such as biological systems.

Antioxidant processes in inhomogeneous systems such as micelle solutions are considered to include the following steps: (i) the transportations of water-soluble antioxidants and free radical to the reaction-progressing region in micelle and (ii) the reaction step between free radicals and antioxidants. The observation of these steps is considered to be important for a detailed understanding of the antioxidant mechanism in inhomogeneous media. Using photoinitiators and a time-resolved technique in place of the quick-mixing of the radical and antioxidant solutions may give new insights to the radical-scavenging action in inhomogeneous systems. Aromatic carbonyl compounds are considered to be a model of biological quinone compounds such as plast quinone and vitamin K. The triplet state of carbonyl compounds produced by photoexcitation is known to be very reactive compared with the $ArO^•$ and $Toc^•$ radicals. Xanthone (Xn, Figure 1) is one of the aromatic carbonyl compounds, and there have been a lot of reports on its photoinduced reactions in homogeneous and inhomogeneous systems.[24−28] The rate constants (k_q) of the quenching reaction of the excited triplet state of Xn ($^3Xn^*$) with phenols in organic solvents were reported to be on the order of 10^8 to 10^9 M^{-1} s^{-1}, which is slightly smaller than the diffusion controlled limit. In micelle systems, $^3Xn^*$ is expected to react with water-soluble AsH^- very fast at the water−oil interface region of the micelle because Xn exists in the hydrophobic region of the micelle, similarly to $Toc^•$. An investigation of the antioxidant actions using $^3Xn^*$ as a photoinitiator in micelle systems may clarify the characteristic antioxidant kinetics in inhomogeneous media, such as the transportation of water-soluble antioxidants into or around the surface of the micelle.

In the present work, the photoinitiated antioxidant reaction of Vit-C with $^3Xn^*$ has been studied in the sodium lauryl sulfate (SDS), hexadecyltrimethylammonium chloride (CTAC), and TX-100 micelle solutions at various pH, by using a time-resolved electron paramagnetic resonance (TR-EPR) technique. TR-EPR is a powerful tool for investigating photoinduced reactions, not only because it can detect and identify short-lived intermediate radicals directly, but also because it can observe the chemically induced dynamic electron polarization (CIDEP) phenomena.[29−32] Spin polarization induced on the intermediate radicals due to the CIDEP provides information on the early stage of antioxidant actions within microseconds just after the photoexcitation. The information might correspond to the kinetics at the micelle surface, that is, at the water/oil interface region.

Experimental Section

Ascorbic acid (Vit-C), L-ascorbyl 6-palmitate (As−P), and L-ascorbyl 6-stearate (As−S) (Figure 1) are the special grade reagents commercially available from Wako Pure Chemicals and were used as received. Xn (Wako) was purified by recrystallization from ethanol. SDS, CTAC, and TX-100 are the extra-pure grade reagents commercially available from Nacalai Tesque and were used as received. All buffer solutions were prepared using deionized water purified by a Millipore Q system.[16] The pH of the solutions was adjusted using the following buffers whose concentrations were 0.1 M: pH 2.0−3.0, $CH_3COONa-HCl$; pH 4.0−5.0, $CH_3COONa-CH_3COOH$; pH 6.0−8.0, $Na_2HPO_4-KH_2PO_4$; pH 9.0−11.0, $Na_2CO_3-NaHCO_3$. The concentration of each surfactant molecule in the buffer solutions was kept at 5.0 wt %. The concentrations of Xn and Vit-C in the micelle solutions were kept at 5.0×10^{-4} and 5.0×10^{-3} M, respectively. The solvents and sample solutions were deoxygenated by bubbling of N_2 gas before and during the measurements.

The TR-EPR measurements were carried out at room temperature without field modulation by using a modified X-band EPR spectrometer (JEOL JES-FE2XG), as reported before.[33−35] The TR-EPR spectra at several delay times were recorded by a boxcar integrator (Stanford Research System SR-250) whose gate width was kept at 0.2 μs. Third harmonic generation light (355 nm) from a Nd:YAG laser (Continuum Surelight-I) operating at the repetition of 10 Hz was used for the photoexcitation. The sample solution flowed through a quartz flat cell (optical path: 0.3 mm) in the EPR cavity.

Results and Discussion

(1) Photoreaction in Homogeneous Solutions. Figure 2a shows a TR-EPR spectrum observed for the photoreaction system of Xn (5.4×10^{-3} M) with ascorbic acid (4.9×10^{-3} M) in the mixed solvent (2-propanol/H_2O = 9/1, v/v). Two strong and sharp EPR lines in Figure 2a are assigned to the ascorbate monoanion radical ($As^{•-}$, $g = 2.0053$, $A_{H4}(1H) = 0.199$ mT), which was produced by abstracting a hydrogen from the hydroxyl group at the C(2)-position of the ascorbate anion. The broad spectrum overlapped is due to the Xn ketyl radical ($XnH^•$, $g = 2.0031$). The CW-EPR spectrum obtained during 10 Hz laser excitation is also shown in Figure 2d, which was assigned to the $As^{•-}$ radical ($g = 2.0053$, $A_{H4}(1H) = 0.199$ mT, $A_{H6}(2H) = 0.021$ mT). The $XnH^•$ radical could not be observed in the CW-EPR spectrum, probably due to its short lifetime. The *g*-factor and the hyperfine coupling constants (hfcc's) of these radicals are in good agreement with those in the literature.[36−39] These radicals are considered to be produced by the hydrogen atom transfer (HAT) reaction from Vit-C to $^3Xn^*$, as shown in Scheme 1.

The E*/A (low-field side emission/high-field side absorption with excess emission) pattern of the spectrum shown in Figure 2a can be explained by the superposition of the triplet mechanism (TM) and the ST_0 mixing of the radical pair mechanism (RPM).[29−32] The interaction of the ST_0 mixing of the RPM between $XnH^•$ and $As^{•-}$ radicals produces an E/A type polarization, and the relatively large difference in *g* factor (Δg) between $XnH^•$ and $As^{•-}$ radicals induces the excess emissive polarization to the $As^{•-}$, and the excess absorptive polarization to the $XnH^•$. The TM polarization produced in $^3Xn^*$ by the anisotropic intersystem crossing should give both radicals net emissive

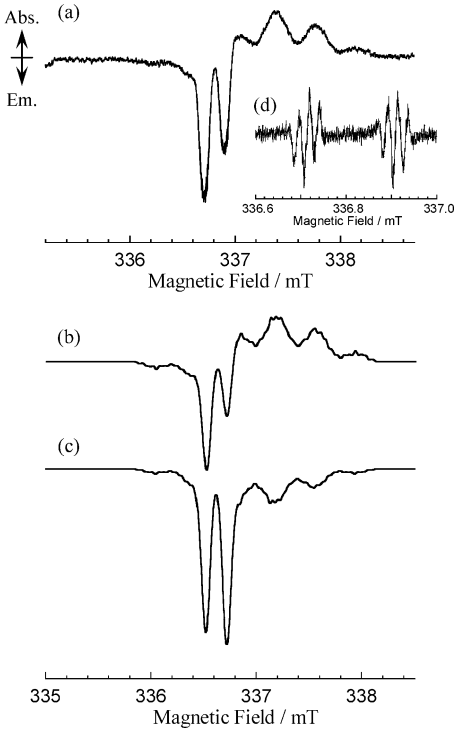

Figure 2. (a) TR-EPR spectrum obtained by the photoreaction of Xn with Vit-C in the mixed solvent (2-propanol/H_2O = 9/1, v/v) at room temperature. The delay time is 1.0 μs. The simulated spectra assuming that the spin polarization is produced by (b) pure TM and (c) pure RPM are also shown. Parameters used in the simulation are given in the text. (d) A CW-EPR spectrum observed in this system during 10 Hz laser excitation using 100 kHz field modulation.

SCHEME 1

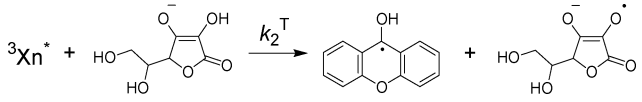

polarization. Parts b and c of Figure 2 show the spectra simulated by assuming that the spin polarization is produced by pure TM and pure RPM, respectively. The observed spectrum can be well reproduced by superposing these TM and RPM spectra.

The TM contribution in the spectrum increases with increasing the concentration of Vit-C, because the faster reaction can conserve a larger amount of the TM polarization to the radicals as a result of the competition of the reaction and the spin−lattice relaxation in the triplet state. A magnitude of the TM polarization (P_{TM}) is represented by[40,41]

$$P_{TM} \propto \frac{k_T {}^3T_1}{1 + k_T {}^3T_1} \qquad (1)$$

$$k_T = k_2{}^T[\text{Vit-C}]$$

where $^3T_1$ and $k_2{}^T$ denote a spin−lattice relaxation time and a second-order quenching rate constant of the triplet state, respectively. Figure 3 shows the P_{TM} vs k_T plot, using the value of $^3T_1 = 6 \times 10^{-9}$ s of ^{3}Xn* obtained in 2-propanol.[28] The RPM polarization can be assumed to be independent of the quenching reaction rate. Therefore, the ratio of the contribution of the TM to the RPM polarization (P_{TM}/P_{RPM}), which is estimated by the spectral simulation, is considered to be approximately proportional to P_{TM}. From the P_{TM}/P_{RPM} obtained from the spectra measured under the conditions of several Vit-C concentrations, the second-order rate constant ($k_2{}^T$) of the

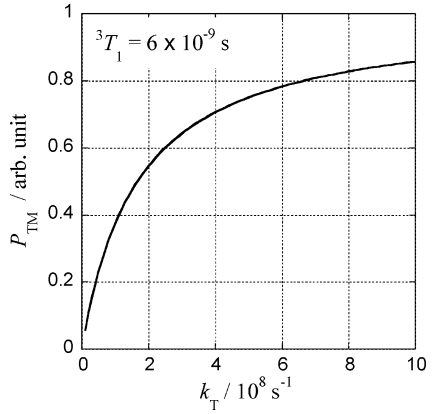

Figure 3. k_T dependence of the P_{TM} value calculated by assuming $^3T_1 = 6 \times 10^{-9}$ s.

reaction of ^{3}Xn* with AsH^- was estimated to be 1.5×10^9 M^{-1} s^{-1}. This value is slightly smaller than the diffusion-control limit of 2-propanol and is comparable to those reported for other photoreaction systems.[27,42]

(2) pH Dependence of the Photoreaction in the Micelle Solutions. Figure 4 shows the TR-EPR spectra observed in the photoreaction of Xn (5.0×10^{-4} M) with ascorbic acid (5.0×10^{-3} M) in the CTAC, SDS, and TX-100 micelle solutions at pH 2−11. As in homogeneous solutions, the spectra were assigned to those of the $As^{\bullet -}$ and $XnH^{\bullet}$ radicals, except for the spectra at pH > 10 in the TX-100 system, in which Xn anion radical was observed in place of $XnH^{\bullet}$. This will be due to the dissociation of the hydroxyl proton from $XnH^{\bullet}$ at pH > 10. The reaction of ^{3}Xn* with TX-100 molecule was not observed in the present systems. These results indicate that the photoinduced antioxidant reaction of Vit-C against ^{3}Xn* successfully proceeded in the micelle systems at the pH 2−10. The spectral pattern and the signal intensities were dependent upon the kind of micelles and pH of the solutions. These dependences seem to be related to the antioxidant kinetics in the micelle systems.

In the TX-100 system, the contribution of the net emissive component in the spectrum was so large that the spectrum can be almost reproduced by assuming only the TM polarization. On the other hand, the contribution of the TM polarization was relatively small in the SDS and CTAC micelle systems. These results indicate that the quenching reaction rate of ^{3}Xn* with Vit-C varies remarkably depending on the micelle systems used. From the large TM contribution in the TX-100 system, the quenching reaction rate of ^{3}Xn* with Vit-C is considered to be as large as the $1/^3T_1$ of ^{3}Xn*, whereas the very small TM contribution in the SDS system suggests that the reaction rate of ^{3}Xn* with Vit-C is less than $1/^3T_1$. The P_{TM}/P_{RPM} values estimated by the spectral simulation were almost constant at pH 2−11 in each micelle system. It is considered that ^{3}Xn* is so reactive that the small difference in quenching reactions due to the pH change is not observed by the present method. The values of P_{TM}/P_{RPM} estimated were 0.43 in CTAC, 0.33 in SDS, and >10 in TX-100. Assuming that the relation between P_{TM}/P_{RPM} and k_T in the micelle systems is the same as that in 2-propanol/H_2O, the quenching reaction rate constants (k_T) at the present Vit-C concentration were estimated to be $\sim 3 \times 10^7$ s^{-1} in CTAC, $\sim 10^7$ s^{-1} in SDS, and more than 10^8 s^{-1} in TX-100. These k_T values are larger than that estimated for the 2-propanol/H_2O system (7.5×10^6 s^{-1}) under the conditions of the same Vit-C concentration. The large quenching rate obtained in the TX-100 system suggests that the HAT reaction occurs inside the micelle. Therefore, Vit-C should exist in the inner region of the micelle together with ^{3}Xn*. The slower rate

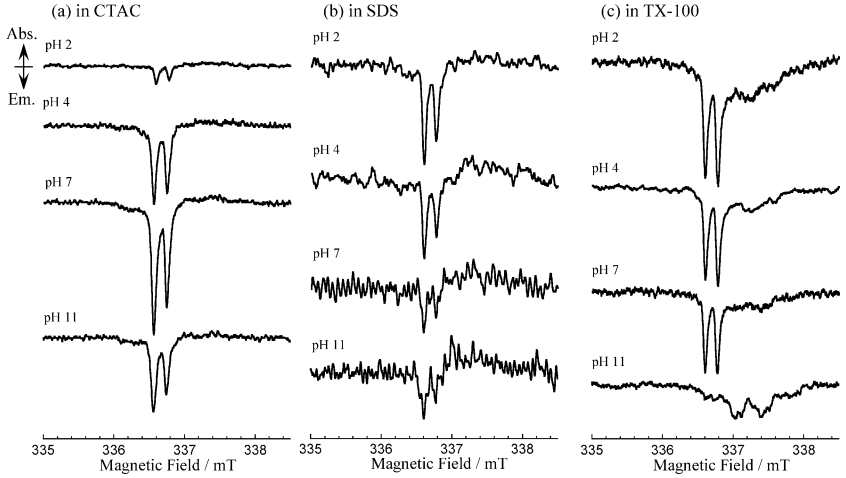

Figure 4. TR-EPR spectra obtained by the photoreaction of Xn with Vit-C in (a) CTAC, (b) SDS, and (c) TX-100 micelle solutions at pH 2−11. The delay time is 1.2 μs.

constants estimated for the CTAC and SDS systems may suggest that the antioxidant reactions do not occur inside the micelle. The rate constants for ^{3}Xn* exiting from the micelle were reported to be 5.8×10^5 s^{-1} on CTAC and 1.7×10^6 s^{-1} on SDS.[43] The rate constants for ^{3}Xn* displacement from the inside to the surface of the micelle were also reported to be $<5 \times 10^7$ s^{-1} in CTAC and 3.1×10^8 s^{-1} in SDS.[43] The estimated quenching rate in the CTAC system in the present study is the same order of the displacement rate from the inside to the micelle surface for ^{3}Xn*. It suggests that the quenching reaction in CTAC occurs on the surface of the micelle. On the other hand, the quenching rate in the SDS micelle system is smaller than the displacement rate and larger than the exiting rate of ^{3}Xn*. Therefore, the quenching reaction may occur outside of the micelle, but in a region near the micelle.

The signal intensity of the TR-EPR spectrum depends not only on the radical concentration but also on the CIDEP mechanisms, the relaxation processes, the reaction systems, and the experimental conditions such as solvents and temperature, because the signal intensity always varies due to the spin polarization dominated by these factors. In the present study, all of the experimental conditions except for pH were set to be fixed in one micelle system. Therefore, the signal intensities of the radicals in each micelle system are considered to be approximately proportional to the reaction yield. Figure 5 shows the plots for the signal intensity of the Vit-C radical, which is normalized in such a way that the maximum value obtained in the TX-100 system is equal to unity, versus pH in the CTAC, SDS, and TX-100 micelle systems. The pH dependence of the signal intensity varies depending on the micelle systems used. Mole fractions of AsH_2 (undissociated form, broken line), AsH^- (ascorbate monoanion, solid line), and As^{2-} (ascorbate dianion, dotted line) calculated from the reported values of the dissociation constants ($pK_{a1} = 4.17$ and $pK_{a2} = 11.57$)[44] are superimposed in Figure 5. These plots indicate interesting relations between the EPR intensity and mole fractions of three forms of Vit-C.

The maximum signal intensity of the TR-EPR spectra in the CTAC system was the largest of those in the three micelle systems. As shown in Figure 5a, the signal intensity in the CTAC system rapidly increases from 0.4 at pH 2 to 2 at pH 6−8 and rapidly decreases to 1 at pH 11. This pH dependence very much resembles the behavior of k_2 for the reaction between Toc$^\bullet$ and Vit-C (reaction II) obtained by the stopped-flow method,[16] and it is well correlated with the mole fraction of AsH^-. On the other hand, the signal intensities in the SDS micelle system were rather smaller, and its pH dependence was quite different from that in CTAC. As shown in Figure 5b, the intensity reaches a maximum at pH 2−3 and then decreases to about half around pH 5 with the increase of pH. The signal intensity in SDS might be correlated with the mole fraction of AsH_2 rather than that of the AsH^-. In the TX-100 system (Figure 5c), the signal intensity was about half that in CTAC and was

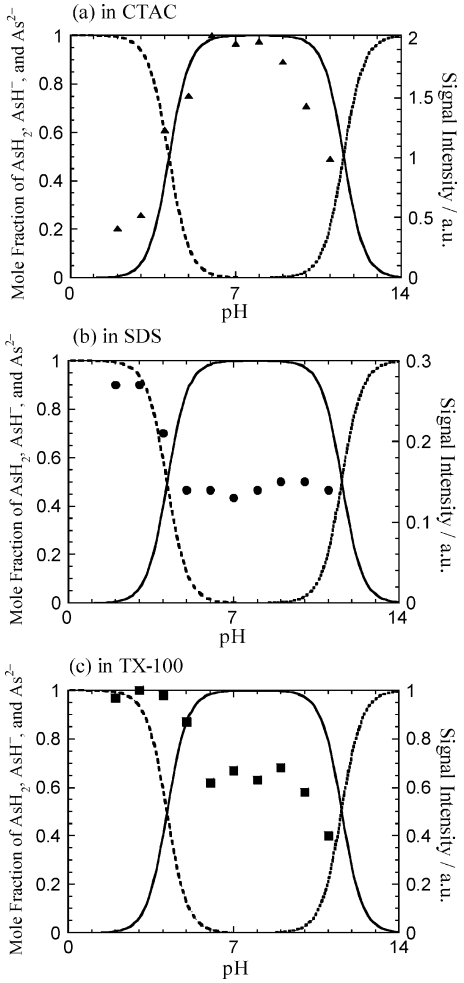

Figure 5. Plots of the relative intensity of the As^- radical in the TR-EPR spectra versus pH in (a) CTAC, (b) SDS, and (c) TX-100 micelle systems. Plots of mole fractions of three Vit-C species (AsH_2, broken line; AsH^-, solid line; As^{2-}, dotted line) versus pH are also shown.

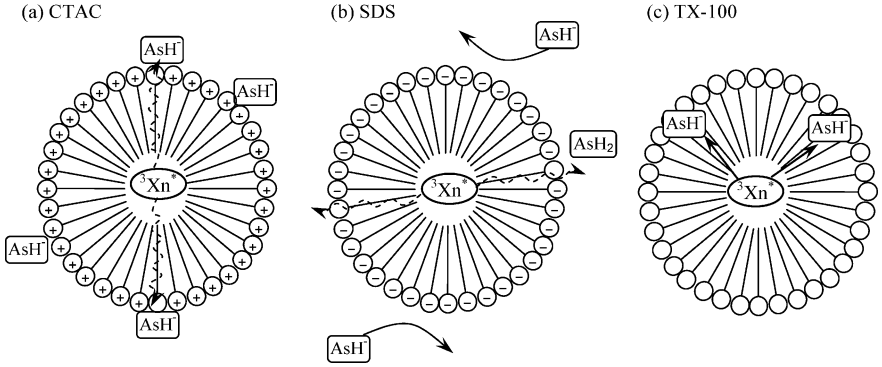

Figure 6. Outline figure of the antioxidant reaction between ^{3}Xn* and Vit-C in the micelle systems.

largest pH 2−3. It decreases to 60% around pH 6, and then to 40% around pH 11. The pH dependence of the signal intensity can be explained by the combination of the mole fraction of AsH_2 and AsH^-. These results suggest the complex mechanism of the quenching reaction of ^{3}Xn* with Vit-C in the micelle systems.

The outline figures of the present reaction between ^{3}Xn* and Vit-C in the micelle systems are shown in Figure 6. In the CTAC systems, the quenching reaction of ^{3}Xn* is considered to progress mainly on the surface of the micelle, as described before. The large signal intensity and the estimated reaction rate in this system support this model. The positive charge at the cationic CTAC micelle surface may attract negative charge species such as AsH^- and As^{2-}, which may adsorb on the micelle surface. Therefore, after the photoexcitation, ^{3}Xn* molecules move from the inside to the surface of the micelle and react quickly with AsH^- or As^{2-} on the micelle surface (Figure 6a). Neutral AsH_2 has less reactivity because it is not attracted to the surface of the CTAC micelle. The pH dependence also indicates that AsH^- has a larger activity than As^{2-} for the present HAT reaction.

In the SDS systems, the quenching reaction of ^{3}Xn* by Vit-C does not occur either inside or on the surface of the micelle, because of the coulomb repulsion between negative charges of the anionic SDS micelle surface and AsH^- or As^{2-}. As a result, the quenching reaction by Vit-C in the SDS micelle system may be less efficient than those in homogeneous solutions. The reaction of ^{3}Xn* with AsH^- or As^{2-} requires the exit of ^{3}Xn* to the outside of the micelle. However, the estimated k_T value for the SDS system is slightly larger than that in 2-propanol/H_2O. The reason for this can be explained in the following way. As shown before, the pH dependence of the signal intensity correlated with the mole fraction of AsH_2 suggests that the quenching reaction of ^{3}Xn* in the SDS system proceeds most efficiently with AsH_2 than with the other forms of Vit-C. Because the neutral AsH_2 can approach the SDS micelle, AsH_2 has more possibility to react with ^{3}Xn* than AsH^- and As^{2-} (Figure 6b). As described above, the estimated k_T in the SDS system is slightly larger than the reported rate constant[43] of the exit of ^{3}Xn* from the micelle. The reason for this is that the present TR-EPR method selectively observes the process around the water/oil interface region of the micelle.

As described before, the quenching reaction of ^{3}Xn* by Vit-C in the neutral TX-100 system occurs mainly inside the micelle. In the TX-100 system, the large signal intensity and the large TM contribution indicate a faster quenching reaction than those in the homogeneous solutions. The lack of the observation of the spin-correlated radical pair may suggest the quick exit of the $As^{\bullet -}$ radical to the water phase from the micelle. The pH dependence of the signal intensity in the TX-100 system is explained in terms of the contribution of AsH_2 and AsH^- in the quenching reaction. The result suggests that the reaction yield is controlled by the amount of AsH_2 and AsH^- taken into the micelle (Figure 6c). It is well-known that the charged species are difficult to exist in the hydrophobic region of the micelle and tend to be extracted in the water phase. Therefore, the ease of incorporation inside the micelle increases in the order $As^{2-} < AsH^- < AsH_2$. As a result, the reactivity also increases in that order.

These results suggest that the rate of the quenching reaction of ^{3}Xn* by Vit-C in the micelle systems is controlled by two values, that is (i) the amounts of Vit-C incorporated in the reaction-progressing region around water−oil interface of the micelles and (ii) the quenching rate, which depends largely on the dissociation forms of Vit-C. Point (i) is related to the fact that only the short-distance quenching is effective in the present system because of its short lifetime of ^{3}Xn* and relatively high viscosity of the micelle inside. As described before, the k_2 value of the 5,7-diisopropyltocopheroxyl radical (5,7-di-^{i}PrToc$^\bullet$) by Vit-C determined by the stopped-flow technique in 2-propanol/H_2O (5:1, v/v) was 25 times as large as that in the TX-100 micelle solution. The reason for this can be explained in the following way. In the stopped-flow experiments, the reaction started by mixing a radical solution and an antioxidant solution. After mixing, Vit-C is required to diffuse to the reaction-progressing region of the micelle containing 5,7-di-^{i}PrToc$^\bullet$ for the quenching reaction. (On the other hand, in the present TR-EPR experiments, both Xn and Vit-C exist in the TX-100 micelle before photoinitiation.) The amount of Vit-C diffused into the micelle is considered to be much smaller than the total Vit-C concentration of the solution. Therefore, the k_2 value in the micelle system was smaller than that in homogeneous solution (2-propanol/H_2O). Furthermore, ubiquinol-10 and ascorbate show similar rate constants ($k_2 = 5.33 \times 10^4$ and 6.32×10^4 M^{-1} s^{-1}) for the reaction with 5,7-di-^{i}PrToc$^\bullet$ in homogeneous solution (2-propanol/H_2O), whereas those in TX-100 (pH 7) are very different from each other (9.24×10^5 and 2.49×10^3 M^{-1} s^{-1}). The reason for this is also that the amount of the antioxidant around the reaction-progressing region is different between oil-soluble ubiquinol-10 and water-soluble ascorbate.

(3) Photoreation of L-Ascorbyl 6-Stearate and L-Ascorbyl 6-Palmitate in the Micelle Solutions. To investigate the mechanism of the quenching reaction of ^{3}Xn* by Vit-C in the TX-100 micelle system, L-ascorbyl 6-stearate (As−S) and L-ascorbyl 6-palmitate (As−P) that are oil-soluble fatty acid esters of Vit-C (Figure 1) were used. In the micelle systems, these Vit-C esters are expected to exist in the hydrophobic region of the micelle, together with Xn, because of their hydrophobic chains. The TR-EPR spectra obtained on the photoreaction of

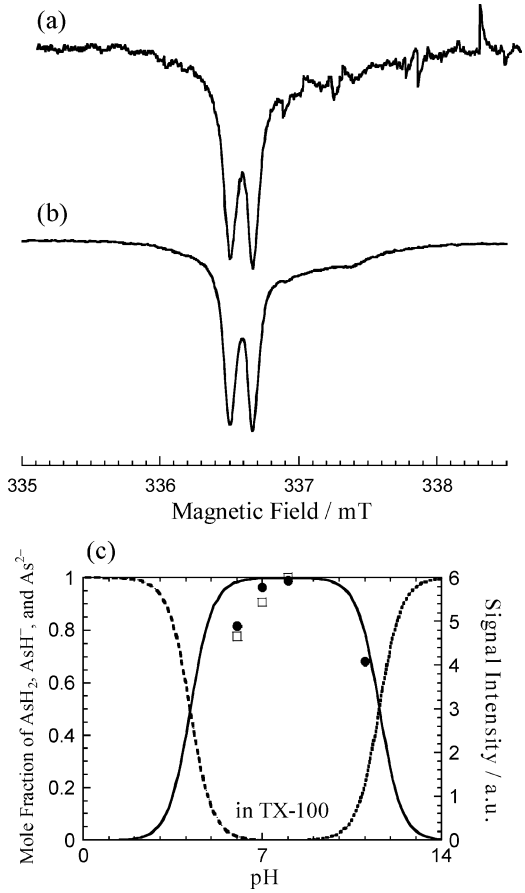

Figure 7. TR-EPR spectra obtained by the photoreaction of Xn with (a) As−P and (b) As−S in a TX-100 micelle solution at pH 6−11. The delay time is 1.2 μs. (c) pH dependence of the relative signal intensity of the As^- radical obtained by the reaction of Xn with As−P (●) and As−S (□) in TX-100 micelle system. The plots of mole fractions of three Vit-C species (AsH_2, broken line; AsH^-, solid line; As^{2-}, dotted line) versus pH are also shown.

Xn with As−S and As−P in the TX-100 micelle are shown in Figure 7a,b. The observed spectra were also assigned to the Vit-C ester and the Xn ketyl radicals. The HAT reaction between ^{3}Xn* and As−S or As−P successfully occurred in the micelle system. No spectral difference between As−S and As−P was observed. The strong signal intensities in these systems, which are 6−10 times as large as those for the water-soluble-Vit-C/TX-100 system (Figure 4c), indicate a very high reaction yield. Furthermore, the net emissive component in the spectra is so predominant that the spectrum can almost be reproduced by assuming only the TM polarization. The value of P_{TM}/P_{RPM} is estimated to be more than 10 and independent of pH. The large quenching rate constant ($>10^9$ s^{-1}) suggests that the HAT reaction occurs inside the micelle, owing to the existence of the hydrophobic chain of the Vit-C esters. The pH dependences of the signal intensity in the As−S/TX-100 and As−P/TX-100 systems are shown in Figure 7c. The pH dependence curves of As−S and As−P resemble that in k_2 obtained by the stopped-flow method, and it is correlated with the mole fraction of the monoanion of the Vit-C esters. However, the estimated pK_a of the Vit-C esters is around 5.5, which is 1−2 times larger than that of Vit-C. The long chain ester group is considered to increase pK_a, because the reaction field of the Vit-C moiety in the Vit-C esters is less hydrophilic than that of ascorbic acid. The results on As−P and As−S indicate that the monoanion form of the Vit-C moiety has the highest HAT reactivity among three different forms of the Vit-C esters. From the present results, it is expected that ~10% of water-soluble Vit-C is taken into the TX-100 micelle at the low pH region and that the reactivity of AsH_2 versus ^{3}Xn* in the TX-100 micelle is 20−50% that of AsH^-. The reactivity of the dianion of the Vit-C moiety is considered to be much smaller than those of the monoanion and undissociated forms.

Conclusion

In the present study, the HAT reaction from Vit-C to ^{3}Xn* in homogeneous and SDS, CTAC, and TX-100 micelle solutions was investigated by the TR-EPR. The TR-EPR spectra assigned to Xn ketyl and Vit-C radicals showed that a fast hydrogen abstraction reaction of ^{3}Xn* from Vit-C progresses in the homogeneous and the micelle solutions. The EPR signal intensity of the Vit-C radical in the micelle systems showed notable pH dependence, which may be due to the acid−base dissociation equilibrium of Vit-C. In homogeneous solutions, the free-radical-scavenging reaction was mainly controlled by the reactivity of antioxidants because both radicals and antioxidants freely diffuse and collide with each other. On the other hand, in inhomogeneous micelle solutions, the reaction was controlled not only by the reactivity of antioxidants but also by the transportation of radicals and antioxidants to the reaction-progressing region, such as around the water−oil interface region of the micelles. Therefore, it is natural to think that a similar situation occurs in biomembranes. The present results clarified the importance of the material transportation of Vit-C to the micelle surface or into the micelle. The difference between the results obtained for Toc• (stopped-flow) and ^{3}Xn* (TR-EPR) might be due to the difference of the reactivity and/or the observation methods. By using the TR-EPR method, we have succeeded in observing the fast reaction of Vit-C against highly reactive ^{3}Xn* in the micelle systems. The results of the present work suggest that the TR-EPR method would be one of the powerful tools for investigating the mechanism of the antioxidant reaction of the natural antioxidants that protect the degradation of the biomembranes.

Acknowledgment. This work was supported by a Grant-in-Aid for the Encouragement of Young Scientists (11740328) from the Japanese Ministry of Education, Science, Sports, and Culture.

References and Notes

(1) Burton, G. W.; Doba, T.; Gabe, E. J.; Hughes, L.; Lee, F. L.; Prasad, L.; Ingold, K. U. *J. Am. Chem. Soc.* **1985**, *107*, 7053.
(2) Burton, G. W.; Ingold, K. U. *Acc. Chem. Res.* **1986**, *19*, 194.
(3) Niki, E. *Chem. Phys. Lipids* **1987**, *44*, 227.
(4) Fukuzawa, K.; Ikebata, W.; Shibata, A.; Kumadaki, I.; Sakanaka, T.; Urano, S. *Chem. Phys. Lipids* **1992**, *63*, 69.
(5) Mukai, K. *Vitamin E in Health and Disease*; Packer, L., Fuchs, J., Eds.; Macel Dekker: New York, 1992; Chapter 8.
(6) *Vitamin E*; Mino, M., Ed.; Japan Scientific Society Press: Tokyo, Japan, 1993.
(7) Mukai, K. *Coenzyme Q: Molecular Mechanisms in Health and Disease*; Kagan, V. E., Quinn, P. J., Eds.; CRC Press LLC: Boca Raton, FL, 2001; Chapter 3.
(8) Packer, J. E.; Slater, T. F.; Willson, R. L. *Nature* **1979**, *278*, 737.
(9) Niki, E.; Tsuchiya, J.; Tanimura, R.; Kamiya, Y. *Chem. Lett.* **1982**, 789.
(10) Niki, E.; Saito, T.; Kawakami, A.; Kamiya, Y. *J. Biol. Chem.* **1984**, *259*, 4177.
(11) Mukai, K.; Watanabe, Y.; Uemoto, Y.; Ishizu, K. *Bull. Chem. Soc. Jpn.* **1986**, *59*, 3113.
(12) Mukai, K.; Morimoto, H.; Okauchi, Y.; Nagaoka, S. *Lipids* **1993**, *28*, 753.
(13) Mukai, K.; Kikuchi, S.; Urano, S. *Biochim. Biophys. Acta* **1990**, *1035*, 77.
(14) Mukai, K.; Nishimura, M.; Ishizu, K.; Kitamura, Y. *Biochim. Biophys. Acta* **1989**, *991*, 276.

(15) Mukai, K.; Nishimura, M.; Nagano, A.; Tanaka, K.; Niki, E. *Biochim. Biophys. Acta* **1989**, *993*, 168.
(16) Mukai, K.; Nishimura, M.; Kikuchi, S. *J. Biol. Chem.* **1991**, *266*, 274.
(17) Mukai, K.; Itoh, S.; Morimoto, H. *J. Biol. Chem.* **1992**, *267*, 22277.
(18) Mukai, K.; Morimoto, H.; Kikuchi, S.; Nagaoka, S. *Biochim. Biophys. Acta* **1993**, *1157*, 313.
(19) Nagaoka, S.; Kuranaka, A.; Tsuboi, H.; Nagashima, U.; Mukai, K. *J. Phys. Chem.* **1992**, *96*, 2754.
(20) Nagaoka, S.; Nishioku, Y.; Mukai, K. *Chem. Phys. Lett.* **1998**, *287*, 70.
(21) Nagaoka, S.; Inoue, M.; Nishioka, C.; Nishioku, Y.; Tsunoda, S.; Ohguchi, C.; Ohara, K.; Mukai, K.; Nagashima, U. *J. Phys. Chem. B* **2000**, *104*, 856.
(22) Mukai, K.; Oka, W.; Watanabe, K.; Egawa, Y.; Nagaoka, S.; Terao, J. *J. Phys. Chem. A* **1997**, *101*, 3746.
(23) Mukai, K.; Kanesaki, Y.; Egawa, Y.; Nagaoka, S. *Phytochemicals and Phytopharmaceuticals*; Shahidi, F., Ho, C.-T., Eds.; AOCS Press: Champaign, IL, 2000; Chapter 20.
(24) Cavaleri, J. J.; Prater, K.; Bowman, R. M. *Chem. Phys. Lett.* **1996**, *259*, 495.
(25) Sakaguchi, Y.; Hayashi, H.; Murai, H.; I'Haya, Y. *J. Phys. Chem.* **1986**, *90*, 550.
(26) Koga, T.; Ohara, K.; Kuwata, K.; Murai, H. *J. Phys. Chem. A* **1997**, *101*, 8021.
(27) Ohara, K.; Hirota, N.; Martino, D. M.; van Willigen, H. *J. Phys. Chem. A* **1998**, *102*, 5433 and references therein.
(28) Ohara, K.; Murai, H.; Kuwata, K. *Bull. Chem. Soc. Jpn.* **1992**, *65*, 1672.
(29) McLauchlan, K. A.; Hore, P. J. *Advanced EPR: Applications in Biology and Biochemistry*; Hoff, A. J., Ed.; Elsevier: Amsterdam, 1989.
(30) McLauchlan, K. A. *Modern Pulsed and Continuous-Wave Electron Spin Resonance*; Kevan, L., Bowman, M. K., Eds.; John Wiley & Sons: New York, 1990; Chapter 7.
(31) van Willigen, H.; Levstein, P. R.; Ebersole, M. H. *Chem. Rev.* **1993**, *93*, 173.
(32) *Dynamic Spin Chemistry*; Nagakura, S., Hayashi, H., Azumi, T., Eds.; Kodansha: Tokyo, Japan, 1998; Chapter 7.
(33) Ohara, K.; Nagaoka, S.; Mukai, K. *Bull. Chem. Soc. Jpn.* **2000**, *73*, 37.
(34) Ohara, K.; Mukai, K. *Chem. Phys. Lett.* **2000**, *317*, 619.
(35) Nishioku, Y.; Ohara, K.; Mukai, K.; Nagaoka, S. *J. Phys. Chem. B* **2001**, *105*, 5032.
(36) Lagercrantz, C. *Acta Chem. Scand.* **1964**, *18*, 562.
(37) Ruf, H. H.; Weis, W. *Biochim. Biophys. Acta* **1972**, *261*, 339.
(38) Ohara, K.; Miura, Y.; Terazima, M.; Hirota, N. *J. Phys. Chem. A* **1997**, *101*, 605.
(39) Wilson, R. *J. Chem. Soc. B* **1968**, 1581.
(40) Ohara, K.; Terazima, M.; Hirota, N. *J. Phys. Chem.* **1995**, *99*, 17814.
(41) Atkins, P. W.; Evans, G. T. *Mol. Phys.* **1974**, *27*, 1633.
(42) Bisby, R. H.; Parker, A. W. *J. Am. Chem. Soc.* **1995**, *117*, 5664.
(43) Mohtat, N.; Cozens, F. L.; Scaiano, J. C. *J. Phys. Chem. B* **1998**, *102*, 7557.
(44) *The Merck Index*, 10th ed.; Windholtz, M., Budavari, S., Blumetti, R. F., Otterbein, E. S., Eds.; Merck & Co., Inc.: Rahway, NJ, 1983.